

- Rice, *Angew. Chem.* **1996**, *108*, 2253; *Angew. Chem. Int. Ed. Engl.* **1996**, *35*, 2116.
- [3] a) C. P. Moore, S. A. VanSlyke, H. J. Gysling (Eastman Kodak), US-A 5484922, **1996**; b) T. Sano, M. Fujita, T. Fujii, Y. Nishio, Y. Hamada, K. Shibata, K. Kuroki (Sanyo Electric Company), US-A 5432014, **1995**; c) Y. Hironaka, H. Nakamura, T. Kusumoto (Idemitsu Kosan Company), US-A 5466392, **1995**; d) S. A. VanSlyke, P. S. Bryan, F. V. Lovecchio (Eastman Kodak), US-A 5150006, **1992**; e) P. S. Bryan, F. V. Lovecchio, S. A. VanSlyke (Eastman Kodak), US-A 5141671, **1992**; f) Y. Hamada, T. Sano, M. Fujita, T. Fujii, Y. Nishio, K. Shibata, *Chem. Lett.* **1993**, 905; g) N. Nakamura, S. Wakabayashi, K. Miyairi, T. Fujii, *Chem. Lett.* **1994**, 1741.
- [4] a) J. Ashenhurst, G. Wu, S. Wang *J. Am. Chem. Soc.* **2000**, *122*, 2541; b) J. Ashenhurst, S. Wang, G. Wu *J. Am. Chem. Soc.* **2000**, *122*, 3528; c) Q. Wu, M. Esteghamatian, N. X. Hu, Z. Popovic, G. Enright, S. R. Breeze, S. Wang, *Angew. Chem.* **1999**, *111*, 1039; *Angew. Chem. Int. Ed.* **1999**, *38*, 985; d) Q. Wu, Y. Tao, M. D'Iorio, S. Wang, *Chem. Mater.* **2001**, *13*, 71; e) Q. Wu, J. A. Lavigne, Y. Tao, M. D'Iorio, S. Wang, *Inorg. Chem.* **2000**, *39*, 5248; f) W. Yang, H. Schmider, Q. Wu, Y. Zhang, S. Wang, *Inorg. Chem.* **2000**, *39*, 2397; g) S. Liu, Q. Wu, H. L. Schmider, H. Aziz, N. X. Hu, Z. Popovic, S. Wang, *J. Am. Chem. Soc.* **2000**, *122*, 3671.
- [5] J. Pang, Y. Tao, M. D'Iorio, S. Wang, *Chem. Mater.* **2001**, submitted.
- [6] S. S. Elmorsy, A. Pelter, K. Smith, *Tetrahedron. Lett.* **1991**, *32*, 4175–4176.
- [7] a) H. B. Goodbrand, N. X. Hu, *J. Org. Chem.*, **1999**, *64*, 670; b) J. Lindley, *Tetrahedron* **1984**, *40*, 1433; c) P. E. Fanta, *Synthesis* **1974**, 1.
- [8] Crystal data for crystal **A**:  $C_{54}H_{39}N_9Cl_6Zn_3 \cdot 3CH_2Cl_2 \cdot 0.25C_6H_6$ , rhombohedral,  $R\bar{3}$ ,  $a = b = 33.517(4)$ ,  $c = 19.167(3)$  Å,  $V = 18647(4)$  Å<sup>3</sup>,  $Z = 12$ . Crystal data for crystal **B**:  $C_{54}H_{39}N_9Cl_6Zn_3 \cdot 3C_6H_6$ , triclinic,  $P\bar{1}$ ,  $a = 13.805(4)$ ,  $b = 14.848(5)$ ,  $c = 17.384(5)$  Å,  $\alpha = 87.208(6)$ ,  $\beta = 88.569(6)$ ,  $\gamma = 77.828(8)^\circ$ ,  $V = 3478.7(18)$  Å<sup>3</sup>,  $Z = 2$ . Data were collected on a Bruker CCD1000 X-ray diffractometer at 24 °C. Structural solution and refinements were carried out using Bruker AXS SHELXTL NT software. Convergence to final  $R_1 = 0.1283$  and  $wR_2 = 0.3320$  by using 10089 reflections and 495 parameters for **A** and  $R_1 = 0.0991$  and  $wR_2 = 0.1079$  by using 16047 reflections and 791 parameters for **B** were achieved. Crystallographic data (excluding structure factors) for the structures reported in this paper have been deposited with the Cambridge Crystallographic Data Centre as supplementary publication no. CCDC-163379 (**A**) and -163380 (**B**). Copies of the data can be obtained free of charge on application to CCDC, 12 Union Road, Cambridge CB2 1EZ, UK (fax: (+44) 1223-336-033; e-mail: deposit@ccdc.cam.ac.uk).
- [9] a) R. H. Prince in *Comprehensive Coordination Chemistry*, Vol. 5. (Eds.: G. Wilkinson, R. D. Gillard, J. A. McCleverty), Pergamon, New York, **1987**, chap. 56.1; b) T. P. E. Auf der Heyde, *Acta Crystallogr. Sect. B* **1984**, *40*, 582; c) M. C. Kerr, H. S. Preston, H. L. Ammon, J. E. Huheey, J. M. Stewart, *J. Coord. Chem.* **1981**, *11*, 111; d) H. W. Smith, *Acta Crystallogr. Sect. B* **1975**, *31*, 2701.
- [10] Fluorescence emission was measured by coupling the modified fiber to a miniature optical-fiber based spectrometer (SF2000, Ocean Optics, Dunedin, FL), which consists of a fixed grating and charge coupled device (CCD) array detector that covers a spectral range of 300 to 1000 nm. An UV light-emitting diode (368 nm, Nichia, San Jose, CA) was used for excitation. The fiber tip was inserted into a 1.1 L sealed flask, and appropriate volumes of various solvent liquids added and allowed to evaporate for gas-phase exposure.
- [11] a) S. Bevers, S. Schutte, L. W. McLaughlin, *J. Am. Chem. Soc.* **2000**, *122*, 5905; b) K. Shirai, M. Matsuoka, K. Fukunishi, *Dyes Pigm.* **1999**, *42*, 95; c) M. Balon, P. Guardado, M. A. Munoz, C. Carmona, *Biospectroscopy* **1998**, *4*, 185; d) J. S. Hinzmann, R. L. McKenna, T. S. Pierson, F. Han, F. J. Kezdy, D. E. Epps, *Chem. Phys. Lipids* **1992**, *62*, 123.
- [12] a) A. Abdelghani, J. M. Chovelon, N. Jaffrezic Renault, C. Veilla, H. Gagnaire, *Anal. Chim. Acta* **1997**, *337*, 225; b) R. Angelucci, A. Poggi, L. Dori, A. Tagliani, G. C. Cardinali, F. Corticelli, M. Marisaldi, *J. Porous Mater.* **2000**, *7*, 197.

## Lamellae-Nanotube Isomerism in Hydrogen-Bonded Host Frameworks\*\*

Matthew J. Horner, K. Travis Holman, and Michael D. Ward\*

The supramolecular organization displayed by surfactant assemblies (SAs) and block copolymers (BCs) is often characterized by various ordered microstructures—spherical, lamellar, hexagonal, and cubic phases—that exhibit different curvatures of a common interface that defines the boundary between dissimilar segments of the molecular components. The ultimate microstructure reflects a delicate balance of forces on opposite sides of the interface.<sup>[1, 2]</sup> Though typically described by smaller length scales, analogous architectures are evident in crystalline small-molecule assemblies,<sup>[3]</sup> such as the hexagonal urea<sup>[4]</sup> and perhydrotriphenylene<sup>[5]</sup> inclusion compounds, supramolecular hydrogen-bonded nanotubes formed by cyclic peptides<sup>[6]</sup> and cyclodextrins,<sup>[7]</sup> high-symmetry metal–organic coordination networks,<sup>[8]</sup> and lamellar organic salts.<sup>[9]</sup> To the best of our knowledge, however, structural isomerism in organic single crystals based on the curvature of a common two-dimensional supramolecular interface is unknown.

We previously reported that, depending on the identity of the organic substituent, guanidinium organomonosulfonates typically crystallize as either bilayered or continuously layered (CL) architectures. The organic substituents form interdigitated arrays between “quasi-hexagonal” hydrogen-bonded sheets of the guanidinium ions (**G**) and sulfonate (**S**) moieties (Figure 1).<sup>[10]</sup> The two architectures differ with respect to the projection of the organic substituents from each **GS** sheet—whereas substituents project from the same side of each sheet in the bilayer form they project from both sides in the CL architecture, thereby accommodating substituents with a larger steric “footprint”. The **GS** sheet can be described as one-dimensional **GS** ribbons fused by hydrogen bond “hinges” that allow the sheets to pucker (about an angle  $\theta_{IR}$ ) in the CL architectures in order to optimize the packing of the organic substituents.<sup>[11]</sup> Guanidinium salts of appropriately chosen organodisulfonates form analogous bilayer and continuous “brick” host architectures in which the organic substituents serve as “pillars” and generate guest-filled inclusion cavities between the **GS** sheets.<sup>[12]</sup> The preference for a given host architecture depends upon the shape and relative sizes of the pillars and guests, the latter behaving as templates that direct the formation of a particular **GS** host architecture.

We have now discovered that guanidinium organomonosulfonates can also form inclusion compounds, with their

[\*] Prof. Dr. M. D. Ward, M. J. Horner, Dr. K. T. Holman  
Department of Chemical Engineering and Materials Science  
University of Minnesota  
Minneapolis, MN 55445 (USA)  
Fax: (+1) 612-626-7805  
E-mail: wardx004@tc.umn.edu

[\*\*] This work was supported by the National Science Foundation (DMR-9908627), in part by the MRSEC Program of the National Science Foundation (DMR-9809364), and the Natural Sciences and Engineering Research Council of Canada (postdoctoral fellowship for K.T.H.).

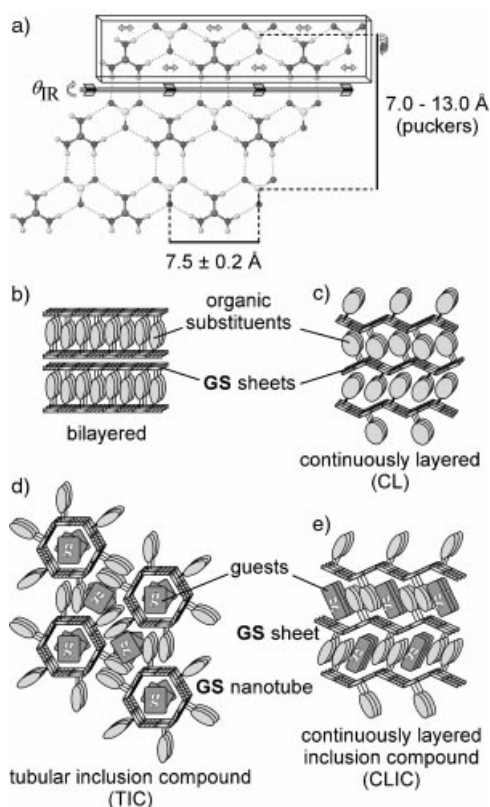
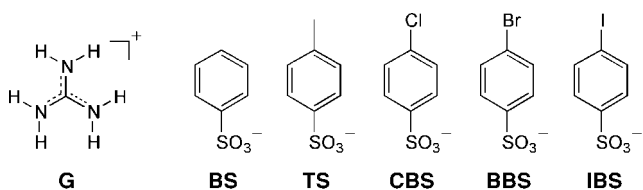


Figure 1. a) Schematic representation of the “quasi-hexagonal” hydrogen-bonded **GS** sheet consisting of 1D ribbons (boxed), which are fused along their edges by hydrogen bond “hinges” about which the sheet can pucker (by an angle  $\theta_{\text{IR}}$ ) in the CL architectures. b–e) Schematic representations of the various architectural isomers of the guest-free and guest-included guanidinium organomonosulfonates.

**GS** frameworks exhibiting bilayered, continuously layered, and hexagonal tubular architectures that are reminiscent of SA and BC microstructures. Guest-free **G**[benzenesulfonate], **G**[*p*-toluenesulfonate], **G**[4-chlorobenzenesulfonate], and **G**[4-bromobenzenesulfonate], herein referred to as **GBS**, **GTS**, **GCBS**, and **GBBS**, respectively, crystallize in the



bilayered form, and **G**[4-iodobenzenesulfonate] (**GIBS**) crystallizes in the CL architecture (Table 1). When crystallization is performed in the presence of certain aromatic molecules, however, these molecules template new **GS** host architectures, either a CL inclusion compound (CLIC) with one guest included per **GS** unit or a tubular inclusion compound (TIC) with two-thirds of a guest per **GS** unit (Figure 1).

The **GS** sheets in the guest-free and inclusion compounds in Table 1 all exhibit identical supramolecular connectivity, that is, the quasi-hexagonal **GS** hydrogen-bonding motif depicted in Figure 1a.<sup>[13]</sup> Therefore, for a given organomonosulfonate the three frameworks can be regarded as architectural

Table 1. Summary of architectures observed in guest-free and guest-included guanidinium organomonosulfonates.

Guest	GBS	GTS	GCBS	GBBS	GIBS
none	bilayer <sup>[a]</sup>	bilayer <sup>[a]</sup>	bilayer <sup>[b]</sup>	<b>bilayer<sup>[b]</sup></b>	CL <sup>[c]</sup>
<i>p</i> -xylene	CLIC <sup>[b]</sup>	CLIC <sup>[b]</sup>	CLIC <sup>[b]</sup>	<b>CLIC<sup>[b]</sup></b>	CLIC <sup>[b]</sup>
<i>m</i> -xylene	TIC <sup>[d]</sup>	CLIC <sup>[b]</sup>	CLIC <sup>[b]</sup>	CLIC <sup>[b]</sup>	CLIC <sup>[b]</sup>
<i>o</i> -xylene	TIC <sup>[c]</sup>	TIC <sup>[c]</sup> /CLIC <sup>[b]</sup>	TIC <sup>[c]</sup>	CLIC <sup>[b]</sup>	CLIC <sup>[b]</sup>
2-chlorotoluene	TIC <sup>[c]</sup>	CLIC <sup>[d]</sup>	TIC <sup>[c]</sup>	<b>TIC<sup>[b]</sup></b>	CLIC <sup>[c]</sup>
1,2-dichlorobenzene	CLIC <sup>[b]</sup>	CLIC <sup>[d]</sup>	TIC <sup>[c]</sup>	TIC <sup>[c]</sup>	CLIC <sup>[d]</sup>
<i>N,N</i> -dimethylaniline	CLIC <sup>[b]</sup>	CLIC <sup>[b]</sup>	TIC <sup>[c]</sup>	TIC <sup>[c]</sup>	CLIC <sup>[b]</sup>

[a] Structures previously reported.<sup>[10a,b]</sup> [b] Completely refined single-crystal structures reported here.<sup>[14]</sup> [c] Assignment based on partially refined single-crystal X-ray diffraction data because of poor quality crystals. [d] Preliminary assignment based upon crystal morphology and <sup>1</sup>H NMR data only. The entries in bold correspond to examples depicted in Figure 2.

isomers. For example, guest-free **GBBS** crystallizes in the bilayered architecture, whereas **GBBS**·(*p*-xylene) and **GBBS**· $\frac{2}{3}$ (2-chlorotoluene) crystallize as a CLIC and TIC, respectively (Figure 2).<sup>[14]</sup> The guests in the CLICs are interdigitated with the organomonosulfonate substituents, thus generating a herringbone motif that resembles the packing commonly observed in single crystals of simple arenes. Rather than forming the guest-free bilayer phase, the added bulk introduced by the guests forces the formation of the CLIC architecture. This effect is similar to the role of bulky organomonosulfonates that promote the formation of guest-free CL phases. The CLICs, similar to the guest-free CL phases, optimize molecular packing through accordionlike puckering of the **GS** sheet, with puckering angles in the range of  $124^\circ < \theta_{\text{IR}} < 144^\circ$ . This puckering affords a lamellar architecture in which the **GS** sheets have zero mean curvature.

In contrast to the CLICs, the **GS** sheets in the TICs exhibit curvature, curling into six-sided *discrete* tubes, each comprising six **GS** ribbons. The tubes assemble into a hexagonal array through dispersive interactions between the organosulfonate substituents that line the outer surface of each tube. The hexagonal symmetry of the nanotubes mandates a puckering angle of  $\theta_{\text{IR}} = 120^\circ$ , which is within the range of values observed for other **GS** compounds. The guest molecules occupy both the tube interior ( $\frac{1}{3}$  guest per **GS** unit) and the region between the tubes (the remaining  $\frac{1}{3}$ ). The guest molecules in the tube are disordered, but the structural data reveal that these guests are stacked cofacially with interplanar separations of approximately 3.8 Å. This value is equivalent to one-half of the *c* lattice constant along the tube, which is defined by the nearest neighbor S...S distance along the **GS** ribbon. The center–center intertube distance is  $d_{\text{tt}} = 16.3$  Å for **GBS** and ranges from 19.2–19.6 Å for the other three hosts. The values reflect the shorter length of the benzene substituent in **GBS**. The inner diameter of the nanotubes, after accounting for the van der Waals radii, is approximately 8 Å. With the exception of **GBBS**· $\frac{2}{3}$ (2-chlorotoluene), crystals of the TICs appear to be slightly twinned and preliminary structural refinements tend to be poor, although assignment of the tubular architecture is unambiguous.

The CLIC and TIC architectures are distinguished by the projection topology of the organic substituents about their

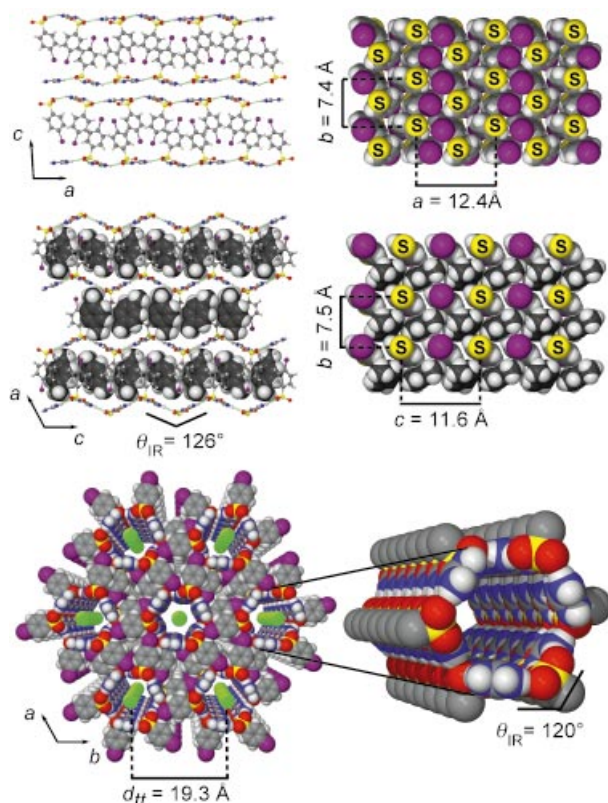


Figure 2. Architectural isomers of the **GBBS** framework. Top: The guest-free bilayer structure as viewed parallel (left) to the hydrogen-bonded **GS** sheets. The packing of the organic substituents between the layers, as viewed normal to the **GS** sheets, is depicted on the right. To better illustrate the packing, the **G** ions and the sulfonate oxygen atoms have been removed and the sulfur atoms labeled. Middle: The CLIC structure observed for  $\text{GBBS} \cdot (p\text{-xylene})$  as viewed parallel (left) to the puckered ( $\theta_{\text{IR}} = 126^\circ$ ) **GS** sheets. The packing of the *p*-xylene guests and the bromobenzene substituents of sulfonate anions are depicted to the right. The sulfur atoms are labeled and the *p*-xylene guests shaded darker. Bottom: The hexagonal packing of the six-sided **GS** nanotubes in  $\text{GBBS} \cdot \frac{2}{3}(2\text{-chlorotoluene})$  as viewed parallel to the long axes of the tubes. For clarity, the guest molecules are depicted as green circles within the nanotubes, but are omitted from the intertube regions. A single nanotube is illustrated on the right. The organic substituents, with the exception of the carbon atom attached to the sulfonate moiety, are removed for clarity. The hydrogen-bonded surface of the nanotube is described by the same quasihexagonal motif as the guest-free and CLIC phases.

respective **GS** sheets. Whereas an equivalent number of organic substituents project from each side of a given sheet in the CLIC architecture, all the substituents in the TIC architecture project outward from the surface of each tube, enforcing curvature of the **GS** sheet and tube formation. The organic substituents on the tube surface exhibit a twofold disorder and suggest herringbone-like packing in the interdigitated regions of adjacent tubes. In general, however, the guests in this region are so highly disordered that an unambiguous assignment of their orientation is not possible.

The three crystal architectures are also reflected in their dramatically different crystal habits, which are illustrated here by the **GTS** phases (Figure 3). The guest-free bilayered crystals form as plates with large (001) faces and the CLICs form rectangular rafts with prominent (010) faces, both forms reflecting fastest growth along the **GS** ribbons (the

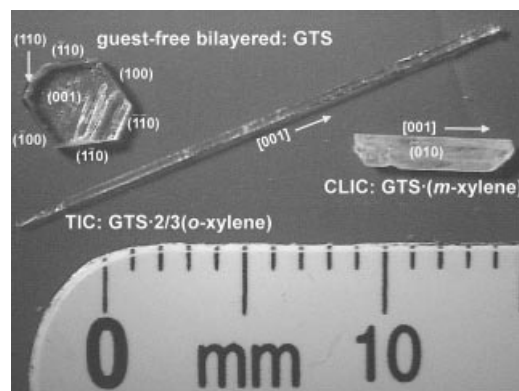


Figure 3. Photograph of single crystals of **GTS**,  $\text{GTS} \cdot (m\text{-xylene})$ , and  $\text{GTS} \cdot \frac{2}{3}(o\text{-xylene})$  which crystallize in the bilayer, CLIC, and TIC architectures, respectively.

[010] direction in the bilayered phase and the [001] in the CLICs). The TICs, however, grow as needles along [001], which coincides with the **GS** ribbons and the long axis of the tubes. Optical microscopy reveals that the tubes have six well-defined sides corresponding to the hexagonal symmetry of the crystals.

Table 1 reveals that the host architecture depends on the specific combination of host and guest. To date, **GTS** is the only host that exhibits both architectures for the same guest (*o*-xylene). Attempts to form inclusion compounds of  $\text{G}[4\text{-fluorobenzenesulfonate}]$  afforded only a guest-free crystalline phase with oblong **GS** tubes wherein two of the fluorobenzene substituents project into the tube interior.<sup>[15]</sup>

The number of examples in this study is not yet sufficient to construct an unambiguous explanation for the preference of the various architectures for specific host–guest combinations. Though kinetic contributions, such as those related to concentration effects, have not yet been thoroughly investigated, the architectural selectivity observed for the CLICs and TICs in Table 1 most likely is governed by subtle differences in the intermolecular packing of the organic substituents and/or guests between the **GS** sheets or tubes. The observation of both a CLIC and TIC for *o*-xylene inclusion compounds of **GTS** suggests similar lattice energies for these architectural isomers. Notably, the host with the largest organomonosulfonate substituent, **GIBS**, only forms CLICs for the guests in Table 1. This may reflect unfavorable steric interactions between the large iodo group and arene rings on adjacent tubes in putative TICs based on this host. Alternatively, the larger iodo substituent may satisfy a dense packing requirement in the CLIC architecture that is not always achieved with hosts endowed with smaller substituents. Inspection of Table 1 suggests that the shape of the guests also plays a role in the selectivity.

The inclusion compounds described here illustrate an architectural isomerism that resembles the morphological behavior observed for SAs and BCs, albeit at a reduced length scale. The isomerism relies on the curvature of a common, flexible yet robust, two-dimensional interface, namely the **GS** sheet. Like SAs and BCs, the energetic penalty for this curvature must be sufficiently small that the hexagonal tube architecture can be achieved.

In principle, the **GS** tubes are expandable because a continuous quasihexagonal tube surface can form with any number of **GS** ribbons greater than three, thereby producing tubes of various diameters<sup>[15]</sup> that can accommodate a range of guest molecules. Molecular models also reveal that tubes constructed from an odd number of ribbons will be chiral. Though it remains to be determined whether volume fraction and frustration models used to explain the microstructures of SAs and BCs can be applied here, we anticipate that the different tube diameters can be achieved through judicious tuning of the steric balance between the guest templates and the organic substituents. The ability to modify the **GS** sheet with different organic substituents provides a distinct advantage over most other organic hosts, which typically cannot be modified in a systematic manner without complete loss of their host architecture. The discrete nature of these self-enclosed nanotubes suggests that, with suitable organic substituents, the isolation of single nanotubes may be possible. The discovery of the new CLIC and TIC architectural isomers, which have substantially different inclusion cavity shapes and dimensionality, also suggests new opportunities in molecular separations<sup>[16]</sup> and materials design.

Received: June 5, 2001 [Z 17220]

- [1] J. M. Seddon, J. L. Hogan, N. A. Warrender, E. Pebay-Peyroula, *Prog. Colloid Polym. Sci.* **1990**, *81*, 189–197.
- [2] a) M. F. Schulz, F. S. Bates, *Phys. Prop. Polym. Handb.* **1996**, 427–433; b) M. W. Matsen, F. S. Bates, *J. Chem. Phys.* **1997**, *106*, 2436–2448.
- [3] B. Moulton, M. J. Zaworotko, *Chem. Rev.* **2001**, *101*, 1629–1658.
- [4] a) M. D. Hollingsworth, K. D. M. Harris in *Comprehensive Supramolecular Chemistry*, Vol. 10 (Eds.: J. L. Atwood, J. E. D. Davies, D. D. MacNicol, F. Vögtle, K. S. Suslick), Pergamon, Oxford, **1996**, pp. 177–237; b) K. D. M. Harris, J. M. Thomas, *J. Chem. Soc. Faraday Trans.* **1990**, *86*, 2985–2996.
- [5] a) M. Farina in *Inclusion Compounds*, Vol. 2 (Eds. J. L. Atwood, J. E. D. Davies, D. D. MacNicol), Academic Press, London, **1984**, pp. 69–95; b) P. J. Langley, J. Hulliger, *Chem. Soc. Rev.* **1999**, *28*, 279–291.
- [6] a) D. T. Bong, T. D. Clark, J. R. Granja, M. R. Ghadiri, *Angew. Chem. Int. Ed.* **2001**, *40*, 1016–1041; *Angew. Chem. Int. Ed.* **2001**, *40*, 988–1011; b) D. T. Bong, T. D. Clark, J. R. Granja, M. R. Ghadiri, *Angew. Chem.* **2001**, *113*, 2221–2224; *Angew. Chem. Int. Ed.* **2001**, *40*, 2163–2166.
- [7] a) W. Saenger in *Inclusion Compounds*, Vol. 2 (Eds.: J. L. Atwood, J. E. D. Davies, D. D. MacNicol), Academic Press, London, **1984**, pp. 231–259; c) G. Gattuso, S. Menzer, S. A. Nepogodiev, J. F. Stoddart, D. J. Williams, *Angew. Chem.* **1997**, *109*, 1615–1617; *Angew. Chem. Int. Ed. Engl.* **1997**, *36*, 1451–1454; d) K. Benner, P. Klufers, J. Schumacher, *Angew. Chem.* **1997**, *109*, 783–785; *Angew. Chem. Int. Ed. Engl.* **1997**, *36*, 743–745.
- [8] a) Z. Xu, Y. H. Kiang, S. Lee, E. B. Lobkovsky, N. Emmott, *J. Am. Chem. Soc.* **2000**, *122*, 8376–8391; b) M. J. Zaworotko, *Chem. Commun.* **2001**, 1–9; c) M. Eddaoudi, D. B. Moler, H. Li, B. Chen, T. M. Reineke, M. O’Keeffe, O. M. Yaghi, *Acc. Chem. Res.* **2001**, *34*, 319–330; d) G. W. Orr, L. J. Barbour, J. L. Atwood, *Science* **1999**, *285*, 1049–1052; e) S. R. Batten, R. Robson, *Angew. Chem.* **1998**, *110*, 1558–1595; *Angew. Chem. Int. Ed.* **1998**, *27*, 1460–1494; f) O. R. Evans, Z. Wang, R. Xiong, B. M. Foxman, W. Lin, *Inorg. Chem.* **1999**, *38*, 2969–2973; g) K. Kasai, M. Aoyagi, M. Fujita, *J. Am. Chem. Soc.* **2000**, *122*, 2140–2141.
- [9] K. Biradha, D. Dennis, V. A. MacKinnon, C. V. K. Sharma, M. J. Zaworotko, *J. Am. Chem. Soc.* **1998**, *120*, 11894–11903.
- [10] a) V. A. Russell, M. C. Etter, M. D. Ward, *J. Am. Chem. Soc.* **1994**, *116*, 1941–1952; b) V. A. Russell, M. C. Etter, M. D. Ward, *Chem. Mater.* **1994**, *6*, 1206–1217; c) V. A. Russell, M. D. Ward, *Acta Crystallogr. Sect. B* **1996**, *52*, 209–214.
- [11] K. T. Holman, A. M. Pivovar, J. A. Swift, M. D. Ward, *Acc. Chem. Res.* **2001**, *34*, 107–118.
- [12] a) V. A. Russell, C. C. Evans, W. Li, M. D. Ward, *Science* **1997**, *276*, 575–579; b) J. A. Swift, A. M. Pivovar, A. M. Reynolds, M. D. Ward, *J. Am. Chem. Soc.* **1998**, *120*, 5887–5894; c) K. T. Holman, S. M. Martin, D. P. Parker, M. D. Ward, *J. Am. Chem. Soc.* **2001**, *123*, 4421–4431.
- [13] Single crystals of the guest-free **GS** phases were grown by evaporation from their methanolic solutions. Single crystals of the inclusion compounds were grown either from methanol solutions containing an excess of the guest or by layering a methanol solution of a **GS** host on neat liquid guest.
- [14] A full hemisphere of data were collected on a Siemens SMART diffractometer with MoK $\alpha$  radiation ( $\lambda = 0.71073$  Å). Data were corrected for absorption, and decay using SADABS. Structures were solved by direct methods (SHELXS) and refined with full-matrix least-squares based on  $|F^2|$  (SHELX-97-2). H atoms were placed in calculated position using a riding model. X-ray data for **GBBS**: C<sub>14</sub>H<sub>20</sub>N<sub>6</sub>O<sub>6</sub>S<sub>2</sub>Br<sub>2</sub>,  $0.36 \times 0.24 \times 0.14$  mm, monoclinic,  $P2_1/c$  (no. 14),  $a = 12.391(1)$ ,  $b = 7.4245(6)$ ,  $c = 26.110(2)$  Å,  $\beta = 95.498(2)^\circ$ ,  $Z = 4$ ,  $V = 2391.0(3)$  Å<sup>3</sup>,  $\rho_{\text{calcd}} = 1.645$  g cm<sup>-3</sup>,  $\mu = 3.605$  mm<sup>-1</sup>,  $1.57 < 2\theta < 27.0^\circ$ ,  $T = 173$  K,  $R_1 = 0.0448$  and  $wR_2 = 0.0943$  for 2907 ( $I > 2\sigma(I)$ ) of 5218 unique reflections and 271 parameters. **GBBS**·(*p*-xylene): C<sub>15</sub>H<sub>20</sub>N<sub>3</sub>O<sub>3</sub>SBr,  $0.45 \times 0.10 \times 0.05$  mm, monoclinic,  $P2_1/n$  (no. 14),  $a = 7.5357(5)$ ,  $b = 20.809(2)$ ,  $c = 11.6326(8)$  Å,  $\beta = 91.463(1)^\circ$ ,  $Z = 4$ ,  $V = 1823.5(2)$  Å<sup>3</sup>,  $\rho_{\text{calcd}} = 1.465$  g cm<sup>-3</sup>,  $\mu = 2.385$  mm<sup>-1</sup>,  $2.0 < 2\theta < 27.0^\circ$ ,  $T = 173$  K,  $R_1 = 0.0387$  and  $wR_2 = 0.0886$  for 2521 ( $I > 2\sigma(I)$ ) of 3971 unique reflections and 210 parameters. **GBBS**· $\frac{2}{3}$ (2-chlorotoluene): C<sub>112/3</sub>H<sub>142/3</sub>N<sub>3</sub>O<sub>3</sub>SBrCl<sub>2/3</sub>,  $0.46 \times 0.22 \times 0.22$  mm, hexagonal,  $P6_3/m$  (no. 176),  $a = b = 19.305(1)$ ,  $c = 7.6998(6)$  Å,  $Z = 6$ ,  $V = 2485.2(3)$  Å<sup>3</sup>,  $\rho_{\text{calcd}} = 1.53$  g cm<sup>-3</sup>,  $\mu = 2.724$  mm<sup>-1</sup>,  $2.4 < 2\theta < 52^\circ$ ,  $T = 173$  K,  $R_1 = 0.0352$  and  $wR_2 = 0.0983$  for 1649 ( $I > 2\sigma(I)$ ) of 1761 unique reflections and 142 parameters. Crystallographic data (excluding structure factors) for the structures reported in this paper have been deposited with the Cambridge Crystallographic Data Centre as supplementary publication nos. CCDC-164111–164126 and -164280–164282. Copies of the data can be obtained free of charge on application to CCDC, 12 Union Road, Cambridge CB2 1EZ, UK (fax: (+44) 1223-336-033; e-mail: deposit@ccdc.cam.ac.uk).
- [15] M. J. Horner, K. T. Holman, M. D. Ward, unpublished results.
- [16] A. M. Pivovar, K. T. Holman, M. D. Ward, *Chem. Mater.* **2001**, *13*, 3018.